

Electronically activated boron-oxygen-related recombination centers in crystalline silicon

Karsten Bothe^{a)} and Jan Schmidt

*Institut für Solarenergieforschung Hameln/Emmerthal (ISFH), Am Ohrberg 1,
D-31860 Emmerthal, Germany*

(Received 9 August 2005; accepted 13 October 2005; published online 3 January 2006)

Two different boron- and oxygen-related recombination centers are found to be activated in crystalline silicon under illumination or electron injection in the dark, both leading to a severe degradation in the carrier lifetime. While one center forms on a time scale of seconds to minutes, the formation of the second center typically proceeds within hours. In order to reveal the electronic and microscopic properties of both defect centers as well as their formation and annihilation kinetics, we perform time-resolved lifetime measurements on silicon wafers and open-circuit voltage measurements on silicon solar cells at various temperatures. Despite the fact that the two centers are found to form independently of each other, their concentrations exhibit the same linear dependence on the substitutional boron (B_s) and quadratic dependence on the interstitial oxygen (O_i) content. Our results suggest that the fast- and the slowly forming recombination centers correspond to two different configurations of a B_sO_{2i} complex. © 2006 American Institute of Physics.
[DOI: 10.1063/1.2140584]

I. INTRODUCTION

The carrier lifetime in boron-doped oxygen-contaminated crystalline silicon is limited by a specific recombination center that forms under illumination or injection of minority carriers in the dark (forward-biased p - n junction). Although already discovered in 1973,¹ detailed investigations to find a conclusive explanation of this material-related effect started not until 1995.² At that time, high-efficiency silicon solar cells were found to degrade under illumination on a time scale of hours^{3–5} by up to 10% relative. As recently reviewed by Schmidt,⁴ the carrier lifetime limiting center responsible for this asymptotic degradation phenomenon is not related to any metal impurities and can always be detected if boron and oxygen are simultaneously present in crystalline silicon.^{3–7} So far, the center has predominantly been studied by means of carrier lifetime measurements. Most attempts to detect the center by other techniques, such as photoluminescence, capacitance spectroscopy, or electron paramagnetic resonance, failed.

Recently, time-dependent open-circuit voltage (V_{OC} - t) and time-resolved carrier lifetime (τ - t) measurements with a time resolution below 0.2 s revealed that the degradation curves are composed of a fast initial decay preceding the slower asymptotic decay^{8,9} (see Fig. 1). Since the activation of the recombination center responsible for the fast initial degradation takes place on a time scale of seconds to minutes, the standard measurement procedures used in the past to investigate the asymptotic degradation process, having a typical time resolution of minutes to hours, have not been able to reveal this fast initial degradation.

In this paper, the fast and the slow degradation process are directly compared. On solar cells and carrier lifetime test structures we show that the defect centers responsible for the

fast as well as for the slow asymptotic degradation are both related to the simultaneous presence of boron and oxygen. However, the fast-forming center is not a precursor of the slowly forming boron-oxygen complex. Furthermore, the stable carrier lifetime after illumination or carrier injection in the dark is shown to be limited by the slowly forming center alone. Despite the fact that different physical mechanisms result in the formation of the two boron-oxygen centers, both defect centers can be deactivated by annealing at 200 °C for 10 min. Interestingly, we find that the annihilation of the fast-forming center proceeds via two stages, whereas the annihilation of the slowly forming center proceeds in one step.

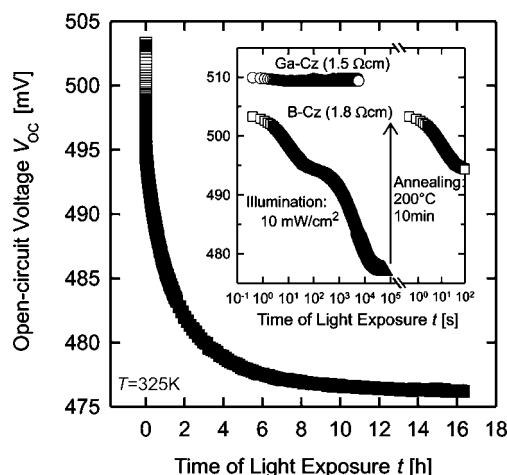


FIG. 1. Measured open-circuit voltage decay due to illumination (halogen lamp with an intensity of 10 mW/cm²) of a MIS n^+ p solar cell made on 1.8- Ω cm B-doped Cz Si. The logarithmic time scale (inset) reveals a fast initial exponential decay, taking place on a time scale of 100 s, followed by a subsequent asymptotic slow decay process. Full recovery of the initial value is possible by annealing at 200 °C for 10 min in the dark. The MIS n^+ p solar cell made on 1.5- Ω cm Ga-doped Cz Si does not show any degradation.

^{a)}Electronic mail: k.bothe@isfh.de

Based on our experimental results we are able to develop an improved microscopic understanding of the complete degradation process, including the fast and the slow component.

II. EXPERIMENTAL DETAILS

The materials under investigation are boron- and gallium-doped Czochralski (Cz) silicon as well as boron-doped magnetically confined grown Czochralski (MCz) and boron-doped float-zone (FZ) silicon wafers from different suppliers. The doping concentration (N_{dop}) is calculated from four-point-probe resistivity measurements at room temperature. N_{dop} can be identified with the acceptor concentration if it is assumed that no thermal donors are present in the material. Interstitial oxygen concentrations $[O_i]$ are determined according to DIN 50438-1 using a Bruker Equinox 55 Fourier transform infrared (FTIR) spectrometer.

Since we intend to analyze bulk recombination centers rather than surface effects, we have to ensure that the recombination activity at the silicon wafer surfaces is minimal. Thus, to keep the surface recombination velocity below 10 cm/s, both surfaces of the samples are RCA cleaned and passivated using plasma-enhanced chemical-vapor deposited (PECVD) silicon nitride films.¹⁰ The passivation quality of these films neither degrades during light exposure nor during temperature treatments below 250 °C. The solar cells under investigation are 300- μm -thick metal-insulator-semiconductor (MIS)-contacted n^+p as well as passivated emitter rear locally diffused (PERL) solar cells.^{11,12}

In order to investigate the dependence of the normalized defect concentrations associated with the fast initial and the subsequent asymptotic degradation on the interstitial oxygen (O_i) and substitutional boron concentrations $[B_s]$, the effective carrier lifetime is measured before (τ_0) and after (τ_d) light-induced degradation by means of the quasi-steady-state photoconductance (QSSPC) method. Since the degradation effect is fully reversible by annealing the samples at 200 °C for 10 min, the initial carrier lifetime τ_0 is measured directly after annealing, while τ_d is measured after illumination with light of a halogen lamp with an intensity of $\sim 10 \text{ mW/cm}^2$. The normalized defect concentration N_τ is then calculated using the expression

$$N_\tau \equiv \frac{1}{\tau_d} - \frac{1}{\tau_0} = \left(\frac{1}{\tau_{\text{SRH}}} + \frac{1}{\tau_{\text{res}}} \right) - \frac{1}{\tau_{\text{res}}}, \quad (1)$$

with τ_{SRH} being the lifetime corresponding to the recombination center under investigation and τ_{res} corresponds to all residual recombination channels including surface recombination. For an accurate determination of N_τ the carrier lifetimes measured to calculate N_τ have to be determined at the same injection level $\eta = \Delta n / N_{\text{dop}}$.¹³

In order to reveal the electronic properties of the activated recombination centers, injection-level-dependent carrier lifetime measurements $\tau(\Delta n)$ are analyzed using the Shockley-Read-Hall (SRH) theory.^{14,15} A fit of the SRH lifetime equation to the experimentally determined lifetime $\tau_{\text{SRH}} = (1/\tau_d - 1/\tau_0)^{-1}$ yields the ratio of the capture cross sections for electrons and holes σ_n/σ_p and the energy level E_t of the recombination center.

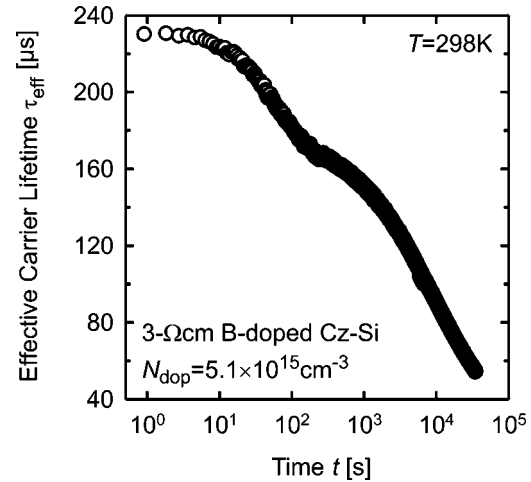


FIG. 2. Effective carrier lifetime of a 3- Ω cm B-doped Cz-Si wafer measured under bias illumination with a halogen lamp with an intensity of 10 mW/cm². The same qualitative decay as shown for the open-circuit voltage in Fig. 1 indicates material-related rather than process-induced recombination centers to be responsible for the degradation process.

The kinetics of the defect formation processes is studied by time-dependent carrier lifetime ($\tau-t$) and open-circuit voltage ($V_{\text{OC}}-t$) measurements. During the $V_{\text{OC}}-t$ measurements the solar cell is held at constant temperature in a liquid-nitrogen-cooled cryostat. In order to access the very initial time range instantaneously after annealing, a data acquisition unit (Agilent 34970A) is used, allowing V_{OC} measurements with a time resolution of 0.2 s and below. During the measurements the solar cell is illuminated with a halogen lamp at an intensity of 10 mW/cm². To avoid any defect formation prior to the $V_{\text{OC}}-t$ measurement, the solar cell is annealed within the cryostat in complete darkness for 10 min at 200 °C.

All $\tau-t$ measurements are performed at or above room temperature using a microwave-detected photoconductance decay (MW-PCD) system (Semilab, WT-2000). This MW-PCD system is equipped with a temperature-controlled sample stage allowing $\tau-t$ measurements in the temperature range of 25–250 °C. Annealing of the samples prior to the $\tau-t$ measurement has to be done on an external hot-plate and requires handling for ~ 10 s under room light conditions. However, as can be seen from Fig. 2, the fast initial degradation can be clearly detected, indicating that the influence of the handling is negligible.

Since the relevant quantity is the normalized defect concentration rather than the carrier lifetime, the time dependence of the defect concentration has to be analyzed. Hence, the measurement $\tau-t$ curves are converted into $N_\tau-t$ curves according to

$$N_\tau(t) \equiv 1/\tau(t) - 1/\tau(t=0). \quad (2)$$

Correspondingly, the results of the $V_{\text{OC}}-t$ measurements on solar cells are converted into $N_{V_{\text{OC}}}-t$ curves using the expression

$$N_{V_{\text{OC}}}(t) \equiv e^{-qV_{\text{OC}}(t)/k_B T} - e^{-qV_{\text{OC}}(t=0)/k_B T}. \quad (3)$$

In order to clarify whether the defect formation is a thermally activated process, the $V_{\text{OC}}-t$ measurements on solar

cells and the τ - t measurements on silicon wafers are performed at various sample temperatures. From the measured data the defect generation rate R_{gen} as well as the activation energy of the defect formation process E_{gen} are determined. The fast and the slow defect formation process are analyzed separately. In the simplest case, the defect formation process follows a single exponential function and thus, the defect generation rate per defect $R_{\text{gen}} \equiv 1/\tau_{\text{gen}}$ can be determined by fitting the equation

$$N(t) = N(t \rightarrow \infty)[1 - \exp(-t/\tau_{\text{gen}})] \quad (4)$$

to the experimental data.

Measuring R_{gen} at different temperatures allows the determination of the thermal activation energy E_{gen} of the defect formation process using the expression

$$R_{\text{gen}}(T) = \kappa_0 \exp\left(-\frac{E_{\text{gen}}}{k_B T}\right), \quad (5)$$

where the pre-exponential factor κ_0 is a characteristic of the physical mechanism of the defect formation.

In order to further elucidate the physical mechanism of the defect formation, we study the V_{OC} degradation of Cz-Si solar cells. The degradation is performed by applying defined forward-bias voltages V_{appl} to the solar cells in the dark. Details of this measurement procedure have already been described in Ref. 16. Knowing the time required to complete the fast and the slow defect formation process, respectively, we are now able to determine the $N_{V_{\text{OC}}}$ values for both defect centers as a function of V_{appl} . The resulting $N_{V_{\text{OC}}}(V_{\text{appl}})$ curves follow a sigmoidal function with a characteristic V_{50} voltage corresponding to the applied voltage necessary to create 50% of the maximum defect concentration. From the temperature dependence of the V_{50} point it is possible to conclude whether the defect activation is due to a simple charge state change process or to a more complex mechanism.

The annihilation of the fast- and the slowly forming centers is investigated separately. The annihilation process of the slowly forming center has been the main focus of two recent studies.^{6,17} After complete activation of the slowly forming center, Rein *et al.*¹⁷ measured the low-injection carrier lifetime of Cz silicon wafers as a function of the annealing time at different temperatures using a MW-PCD system with an integrated cryostat. In contrast to this dynamic approach, Schmidt and Bothe⁶ used a static approach investigating the stable carrier lifetime saturation value of Cz silicon wafers reached under defined temperature and illumination conditions. Under these conditions, annihilation and generation occur simultaneously.

In this work, we study the annihilation of the fast-forming center after applying a defined forward-bias voltage of $V_{\text{appl}}=800$ mV for 10 min in the dark at $T=300$ K to Cz silicon solar cells. This procedure results in a complete fast initial degradation, however, due to its shortness, avoids the subsequent slow degradation process. Thus, the fast-forming defect center is fully activated and the recovery of the open-circuit voltage as a function of temperature can be studied. All V_{OC} measurements are performed at $T=300$ K at an illumination intensity of 10 mW/cm^2 . Since each measurement

takes less than 3 s, the defect formation during the V_{OC} measurement is negligible. During the measurement of each annihilation curve, the samples are cycled between the annihilation and the measurement temperature. In all cases the up and down rampings take less than 4 min.

III. EXPERIMENTAL RESULTS

Figure 1 shows a $V_{\text{OC}}-t$ measurement of a $1.8\text{-}\Omega \text{ cm}$ B-doped Cz-silicon solar cell. The measured open-circuit voltage decreases until a stable level is reached after ~ 16 h. On a logarithmic time scale (see inset of Fig. 1) the complete characteristic of the decay process becomes visible. It is composed of two parts: a very fast initial decay and a subsequent slow asymptotic decay. Solar cells made on Ga-doped Cz-Si or oxygen-lean B-doped FZ silicon do not show any decrease in the open-circuit voltage at all. This is shown in Fig. 1 for a solar cell made on $1.5\text{-}\Omega \text{ cm}$ Ga-doped Cz silicon, which has an O_i content comparable to that of the B-doped solar cell ($[\text{O}_i] \approx 7 \times 10^{17} \text{ cm}^{-3}$). Thus, substituting boron by gallium or avoiding the incorporation of oxygen during the crystal growth results in silicon that is free of any degradation.

In order to exclude any device-related effects, we also perform τ - t measurements on unprocessed B-doped Cz-silicon wafers. As shown in Fig. 2, for a $2.8\text{-}\Omega \text{ cm}$ B-doped Cz-silicon sample, the τ - t measurement clearly confirms the initial fast and subsequent slow degradation.

Since the carrier lifetime degradation can also be observed on intentionally oxygen-contaminated FZ silicon as well as on electronic-grade Cz silicon of highest purity, both known to have extremely low metal contamination levels, the involvement of metal impurities in the degradation is highly unlikely.

A. Oxygen and boron dependences

Figure 3 shows the measured normalized defect concentration N_{τ} determined for the fast- and the slowly forming defect as a function of the substitutional boron concentration $[\text{B}_s]$ for various Cz-Si samples with O_i concentrations in the range of $(7\text{--}8) \times 10^{17} \text{ cm}^{-3}$. As can be seen in Fig. 3, for both processes N_{τ} is proportional to $[\text{B}_s]$. In Fig. 4, N_{τ}/N_{dop} is plotted as a function of the interstitial oxygen concentration $[\text{O}_i]$. Since the proportionality between N_{τ} and N_{dop} allows to investigate N_{τ}/N_{dop} rather than N_{τ} , the database for the analysis of the $N_{\tau}([\text{O}_i])$ dependence can be considerably enlarged as Cz-silicon wafers of various doping concentrations are included. Figure 4 shows the measured data corresponding to the fast- and the slowly forming center together with the fits of a power law $N_{\tau} \sim [\text{O}_i]^{\alpha}$. For both processes we find $\alpha=2$, indicating a quadratic increase of the defect concentration with increasing $[\text{O}_i]$.

B. Electronic properties

As shown in Fig. 5(a), the fast-forming recombination center predominantly affects the carrier lifetime in the low-injection range, whereas the slowly forming recombination center affects the carrier lifetime throughout the entire injection range, shifting the lifetime curve vertically to lower val-

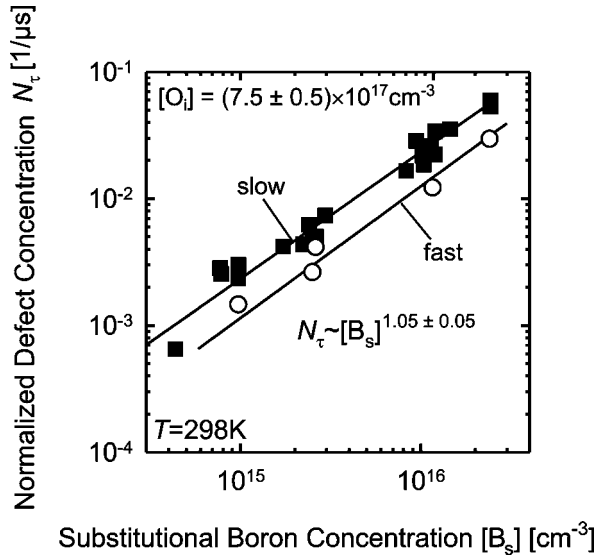


FIG. 3. Measured normalized defect concentrations N_t corresponding to the fast- and the slowly forming recombination center as a function of the substitutional boron concentration $[B_s]$ for Cz-Si wafers of similar oxygen concentrations $[O_i]$. The fitted curves indicate that N_t increases proportionally with $[B_s]$ in both cases. Note that N_t of the fast-forming center is determined at $\eta=0.01$, whereas N_t of the slowly forming center is determined at $\eta=0.1$.

ues. Figure 5(b) shows the SRH lifetimes of the fast- and the slowly forming recombination center determined from the measured carrier lifetime values, together with the fits calculated using the SRH equation. Unfortunately, the injection-level-dependent lifetime measurements alone cannot reveal the exact value of the energy level E_t for defects with an energy level close the middle of the silicon band gap. Thus, the energy level of the fast-forming defect center $E_{t,fast}$ can only be determined to lie between 0.35 and 0.85 eV below the conduction-band edge E_C . On the other hand, the ratio of the capture cross sections for electrons and holes σ_n/σ_p can be determined with a high accuracy to be $\sigma_n/\sigma_p=100\pm10$. This value is one order of magnitude larger than the σ_n/σ_p

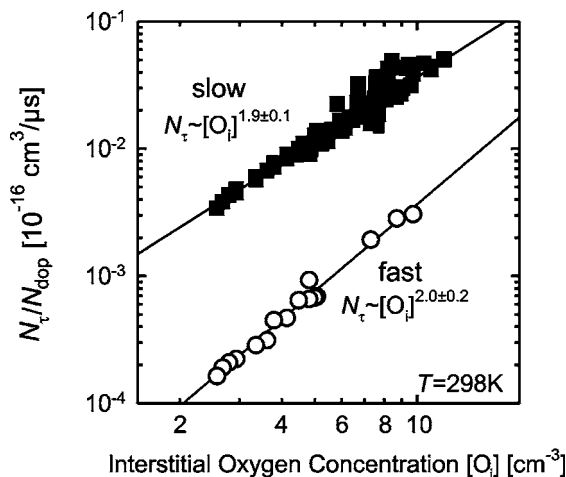


FIG. 4. Measured ratio of the normalized defect concentration N_t to the doping concentration $N_{dop}=[B_s]$ of the fast- and the slowly forming recombination center as a function of the interstitial oxygen concentration $[O_i]$ for more than 40 different Cz-Si samples. The solid lines are fits of a power law showing a quadratic increase of N_t/N_{dop} with $[O_i]$ in both cases.

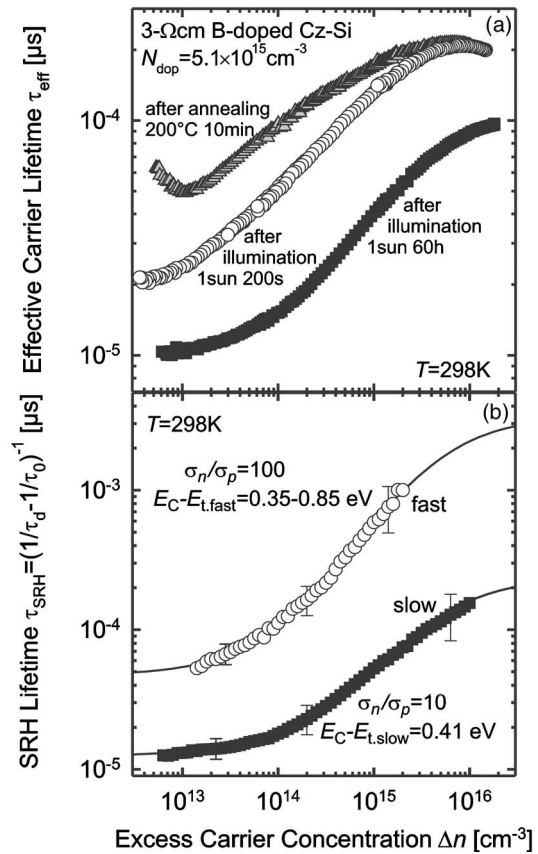


FIG. 5. (a) Measured injection-level-dependent effective carrier lifetime of a boron-doped Cz-Si sample. While the fast-forming center, formed after 200 s of illumination, mainly affects the carrier lifetime in the low-injection range, the slowly forming recombination center affects the lifetime throughout the entire injection range, shifting the curve down to lower lifetime values. (b) Measured and calculated SRH lifetimes, of the fast- and the slowly forming center, respectively. The ratio of the electron-to-hole capture cross sections of the fast-forming center is larger by one order of magnitude compared to that of the slowly forming recombination center.

ratio determined for the slowly forming boron-oxygen complex, indicating a higher electron affinity for the fast-forming center. For the slowly forming center, the electronic defect parameters have already been investigated in detail by different authors and can be regarded as firmly established.^{18,19} Thus, for fitting the injection-level-dependent carrier lifetime after complete activation of the slowly forming recombination center using the SRH theory, the defect energy level $E_{t,slow}$ was set at $E_C-0.41$ eV (Ref. 19) and the capture cross section ratio σ_n/σ_p at 10 ± 1 .^{18,19}

C. Defect formation

Figure 6 shows an Arrhenius plot of the defect generation rate corresponding to the initial fast process $R_{gen,fast}$ as a function of inverse temperature for Cz-Si materials of various boron concentrations. For all samples the measured data points lie on a straight line, clearly proving that the formation process is thermally activated. From the slope of the linear curves shown in Fig. 6, we determine a relatively low barrier energy of $E_{gen,fast}=(0.23\pm0.02)$ eV. The temperature dependence of the defect generation of the slow asymptotic degradation process $R_{gen,slow}$ is shown in Fig. 7. The temperature range investigated in previous studies (open symbols)^{6,20}

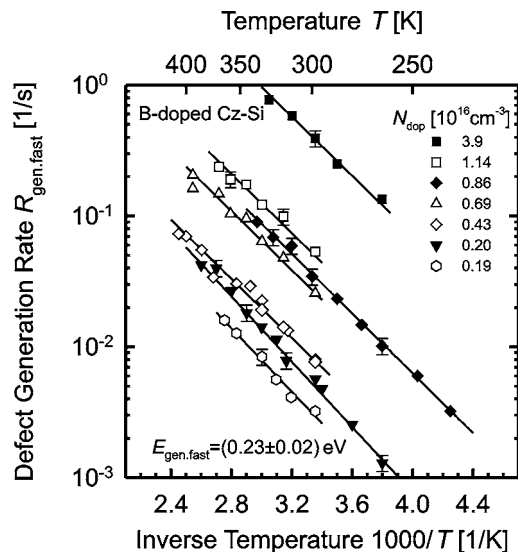


FIG. 6. Measured temperature dependence of the defect generation rate $R_{\text{gen,fast}}$ of the fast-forming center for Cz-Si materials of different doping concentrations N_{dop} . The open symbols refer to the carrier lifetime measurements on silicon wafers, whereas the closed symbols refer to the open-circuit voltage measurements on silicon solar cells.

is extended in order to obtain more reliable data. The circles refer to the open-circuit voltage measurements, whereas the squares refer to the carrier lifetime measurements. For the V_{OC} measurements, the activation of the slowly forming recombination center is realized either by applying a bias voltage in the dark (open circles) or by illumination (closed circles). Isothermal time-dependent carrier lifetime measurements are performed using the QSSPC method (open and closed squares). For both measurement procedures the data points form a straight line in the Arrhenius plot, indicating that the formation of the slowly forming center is also a thermally activated process. While the activation energy $E_{\text{gen,slow}} = (0.475 \pm 0.035) \text{ eV}$ is independent of the boron concentration, the pre-exponential factors are found to increase

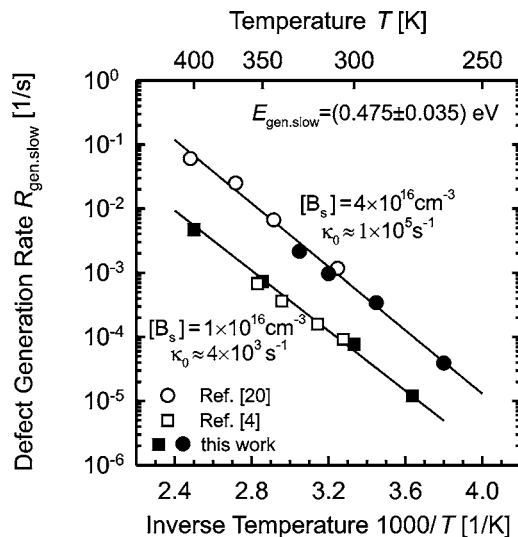


FIG. 7. Measured temperature dependence of the defect generation rate $R_{\text{gen,slow}}$ of the slowly forming center for two Cz-Si materials with different doping concentrations N_{dop} . The open symbols refer to literature data, whereas the closed symbols refer to the data determined in the present work.

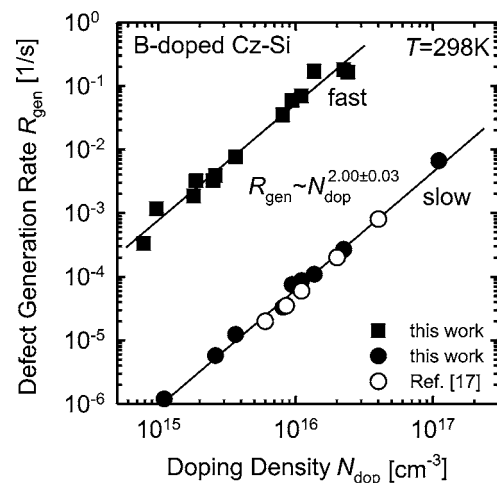


FIG. 8. Measured dependence of the defect generation rate R_{gen} on the doping concentration N_{dop} for the fast- and slowly forming centers, respectively. In both cases the defect generation rate shows a quadratic increase with N_{dop} . The oxygen concentration of the Cz samples ranges from 6 to $8 \times 10^{17} \text{ cm}^{-3}$.

with increasing boron concentration from $\kappa_0 = 4 \times 10^3 \text{ s}^{-1}$ at $[B_s] = 1 \times 10^{16} \text{ cm}^{-3}$ to $\kappa_0 = 1 \times 10^5 \text{ s}^{-1}$ at $[B_s] = 4 \times 10^{16} \text{ cm}^{-3}$.

Investigating the defect formation rates in Cz-Si wafers with different oxygen and boron concentrations by means τ - t measurements reveals an approximately quadratic increase of the defect generation rate with the boron concentration $R_{\text{gen}} \sim [B_s]^2$ (see Fig. 8). This dependence holds for both, the fast as well as for the slow process. Interestingly, for both processes R_{gen} has been found to be independent of the oxygen concentration $[O_i]$ (see Fig. 9). The defect formation is studied in detail by applying different forward-bias voltages V_{appl} to the p - n junction of Cz silicon solar cells and measuring the corresponding V_{OC} decay, as shown for the fast initial process in Fig. 10. The V_{50} values determined from these measurements are shown in Figs. 11 and 12 as a function of temperature for the slow asymptotic and the fast initial process, respectively.

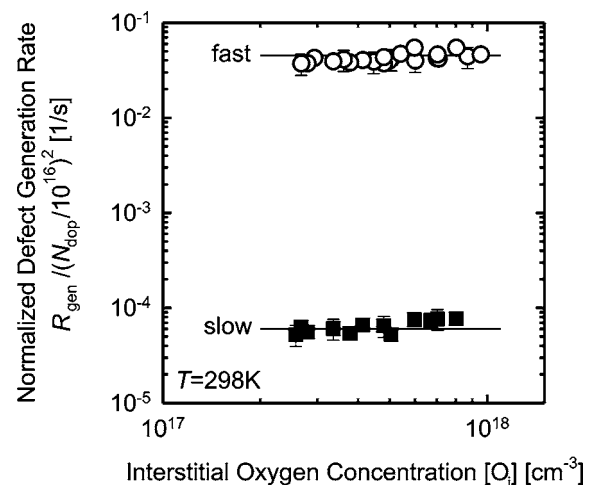


FIG. 9. Measured dependence of the defect generation rate R_{gen} on the interstitial oxygen concentration $[O_i]$ for the fast- and the slowly forming defect centers, respectively. For both centers the defect generation rate does not depend on $[O_i]$.

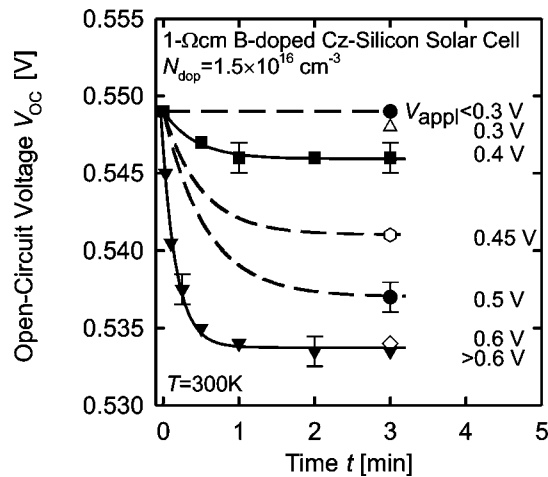


FIG. 10. Forward-bias induced open-circuit voltage degradation curves of an MIS $n+p$ Cz-Si solar cell at different applied voltages V_{appl} . The time for the application of the bias voltage is chosen only to activate the fast-forming recombination center. During each measurement the solar cell is illuminated for only 2–3 s with a halogen lamp of 10 mW/cm² intensity.

D. Defect annihilation

Since the initial state prior to degradation can be completely recovered by annealing, a thermally activated annihilation process may be assumed. This assumption is confirmed by the experimental results shown in Fig. 13. The two different approaches to determine $R_{\text{gen.slow}}$ as a function of temperature by Rein *et al.*¹⁷ and Schmidt and Bothe⁶ yield the same result. From a fit to the measured data, an activation energy of $E_{\text{ann.slow}} = (1.32 \pm 0.05)$ eV is obtained for the annihilation process of the slowly forming recombination center. A further analysis of the pre-exponential factor κ_0 gives a value of $\sim 10^{13} \text{ s}^{-1}$.

Investigating the annihilation of the fast-forming recombination center reveals a more complex behavior. As shown in Fig. 14, for temperatures below ~ 330 K a complete annihilation cannot be achieved within 10^6 s. Furthermore, the annihilation process seems to saturate at an intermediate

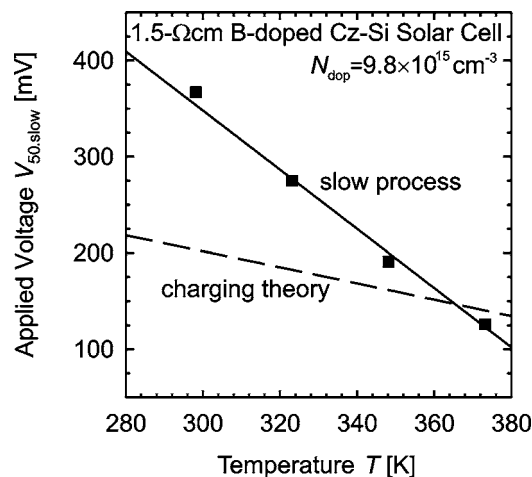


FIG. 11. Measured threshold voltage V_{50} of the slowly forming center in comparison with the expected curve (dashed line) for a charging model, which assumes that the activation of the recombination center occurs by shifting the electron quasi-Fermi level across the energy level of a latent defect.

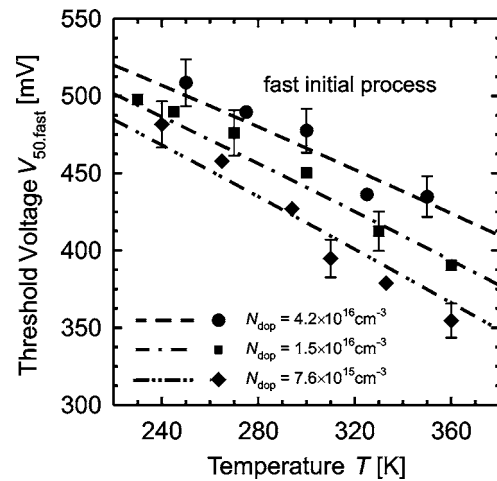


FIG. 12. Measured temperature dependence of the characteristic V_{50} value of the fast-forming center (applied voltage necessary to create 50% of the maximum defect concentration) and calculated $V_{50}(T)$ curves expected for a defect activation due to a charge-state change following from the shift of the electron quasi-Fermi level across a defined energy level of the latent defect. For all three solar cells, experiment and theory agree well for an energy level of the latent state $E_{\text{lat}} = E_v + (635 \pm 20)$ meV obtained from the sum of the Fermi level and the applied voltage $E_{\text{lat}} = E_F + qV_{50}$.

level. The saturation is supported by the annealing results obtained between 375 and 400 K. In this temperature range, the annihilation process proceeds via two stages. While during the first stage an intermediate state is reached, a complete recovery of the initial state is obtained during the second stage. The defect annihilation rates corresponding to stages 1 and 2 are shown in Fig. 15 as a function of temperature. While the first stage is characterized by a low activation barrier of $E_{\text{ann.fast.1}} = (0.32 \pm 0.02)$ eV and a preexponential factor of $\kappa_0 \approx 10^3 \text{ s}^{-1}$, the activation energy of the second stage is found to be $E_{\text{ann.fast.2}} = (1.36 \pm 0.08)$ eV with $\kappa_0 \approx 10^{13} \text{ s}^{-1}$.

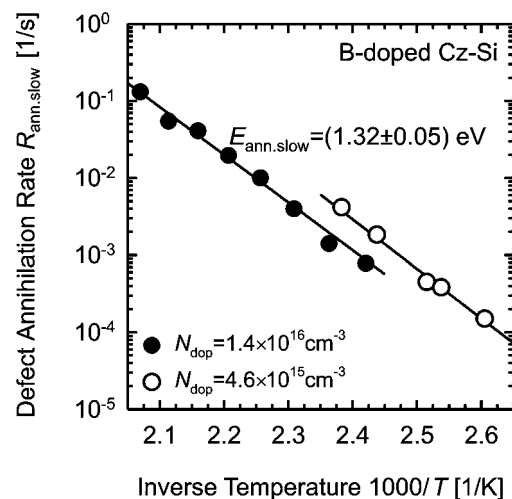


FIG. 13. Arrhenius plot of the defect annihilation rate $R_{\text{ann.slow}}$ of the slowly forming defect center. The same linear dependence found for the two Cz-Si samples with different doping densities clearly indicates that the defect annihilation is a thermally activated process with an energy barrier of $E_{\text{ann.slow}} = 1.32$ eV. An attempt frequency of $\kappa_0 \approx 10^{13} \text{ s}^{-1}$ suggests a diffusion-limited process. Data points shown as closed circles are taken from Ref. 6, whereas data points shown as open circles have been published in Ref. 17.

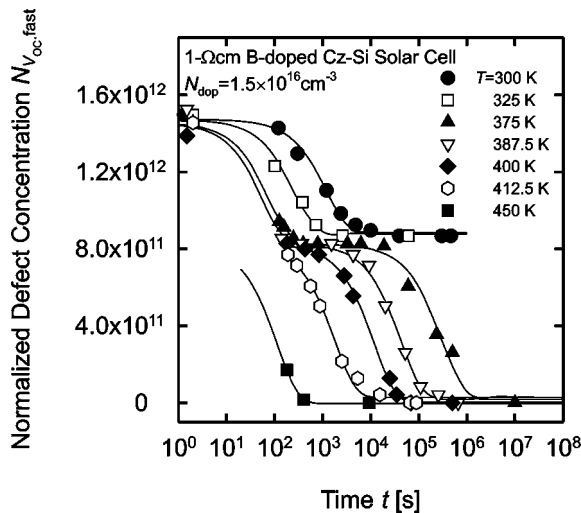


FIG. 14. Measured decrease of the normalized defect concentration $N_{VOc,fast}$ of the fast-forming center as a function of temperature. For temperatures below 330 K a complete annihilation cannot be achieved within 10^6 s. In the temperature range of 375–400 K, the annealing curve is composed of two stages. During the first stage, an intermediate state is reached, while during the second stage a complete annihilation of the fast-forming center occurs. For temperatures below 330 K the characteristic time for the occurrence of the second process is too large to be detectable within the maximum measurement time of 10^6 s, whereas for temperatures above 425 K the characteristic time constant of the first process becomes too small to be detectable.

IV. DISCUSSION

A. Asymptotic degradation

The slow asymptotic degradation process has been widely studied in the past and the defect center made responsible for the process has been studied experimentally^{2–9,13,16–22,27} as well as theoretically.³⁰ As can be seen from Fig. 3, the measured defect concentration N_τ increases linearly with $[B_s]$, which is in excellent agreement with the results of previous studies^{5,7,18,21} of the slowly form-

ing center. In Fig. 4, N_τ/N_{dop} is plotted as a function of $[O_i]$ with the straight line being a fit of a power law $N_\tau \sim [O_i]^\beta$ with $\beta = (1.9 \pm 0.1)$ to the measured data. This quadratic increase is in perfect agreement with our previously published data,⁶ with the extended database resulting in a decrease of the uncertainty range of β . The quadratic dependence of the defect concentration on the interstitial oxygen concentration is a much weaker dependence compared to that found by Glunz *et al.*⁵ in an earlier study. However, in the meantime the latter group re-examined the oxygen dependence of the defect concentration and was able to confirm our finding of a quadratic $N_\tau([O_i])$ dependence.⁷ In their previous study,⁵ an unavoidable systematic error occurred due to the use of constant bias light conditions rather than constant injection level conditions during the carrier lifetime measurements. Furthermore, compared to our data shown in Fig. 4 the $N_\tau([O_i])$ data in Ref. 5 were determined for a very narrow interstitial oxygen range and showed an extremely large scatter. The physical origin of this scatter is still under debate. As has been shown recently,²² the presence of thermal donors (TDs) is one potential source of error. The resistivity due to the doping with boron is considerably reduced by the presence of TDs. As a consequence, the determination of the doping concentration from four-point-probe measurements underestimates the true boron concentration. Depending on the TD concentration, this effect leads to a large error in the determination of the normalized defect concentration, especially for lowly doped silicon.

Rein *et al.*⁷ argued that the strong scatter in their $N_\tau([O_i])$ data might indicate an indirect involvement of interstitial oxygen and proposed intrinsic point defects such as vacancies or self-interstitials as possible candidates interacting with the substitutional boron atoms. However, vacancies have already been ruled out by the same authors⁷ and silicon self-interstitials have more recently been proven to have no impact on the boron-oxygen-related defect concentrations.²³ Thus, assuming the asymptotic lifetime degradation to be due to a defect reaction rather than a change in the atomic configuration of a latent defect complex, the measured $N_\tau([B_s], [O_i])$ dependence suggests a reaction of a cluster of oxygen atoms and one substitutional boron atom. Since substitutional boron is largely immobile in the silicon lattice up to relatively high temperatures, we assume the oxygen dimer (O_{2i}), known to be a very fast diffuser in silicon,^{24,25} to be the oxygen-related part of the defect center responsible for the slow degradation process in B-doped crystalline silicon. The fast-diffusing oxygen dimers are captured by the substitutional boron B_s , forming a B_sO_{2i} complex that acts as a highly recombination-active defect center.⁶ A unique feature of the oxygen dimer is its ability to exist in noticeable concentrations up to 10^{14} cm⁻³ at high temperatures up to the silicon melting point. Thus, the IR absorption at 1012 cm⁻¹ associated with the oxygen dimer can still be detected after high-temperature heat treatments,²⁶ indicating that noticeable oxygen dimer concentrations are always present in oxygen-rich silicon. Furthermore, for the quasi-equilibrium concentration of the oxygen dimer $[O_{2i}]_{eq}$, a quadratic dependence upon $[O_i]$ has been found²⁴ which is in good agreement with

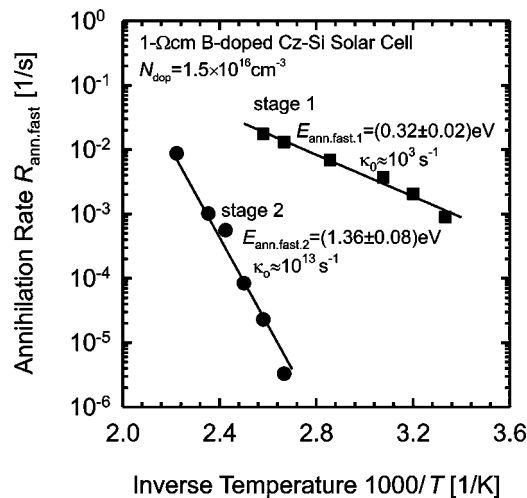


FIG. 15. Arrhenius plot of the defect annihilation rates corresponding to the two stages of the annihilation process of the fast-forming center. Both processes are thermally activated with different activation energies. While the energy barrier of the first process is only $E_{ann,fast,1} = 0.32$ eV, the barrier of the second process is $E_{ann,fast,2} = 1.36$ eV. From the determined preexponential factors κ_0 a diffusion-limited process is probable for stage 2, whereas for stage 1 it can be ruled out.

our B_sO_{2i} model and the experimental results of a nearly quadratic increase of N_τ with $[O_i]$.

The defect formation of the slowly forming boron-oxygen complex is studied in Fig. 7. Our temperature-dependent measurements of the defect generation rate prove that the formation process is thermally activated, with an activation energy of $E_{\text{gen}} = (0.475 \pm 0.035)$ eV. In our B_sO_{2i} model, this energy corresponds to the diffusion barrier of the oxygen dimer.⁶ The measurements shown in Fig. 7 also reveal that the degradation is carrier-induced rather than photon induced. Further information on the impact of the carrier density on the defect formation has been obtained by investigating the defect formation rate as a function of light intensity. As has been shown recently for a Cz-Si sample with a doping concentration of $9.8 \times 10^{15} \text{ cm}^{-3}$,⁶ the defect generation $R_{\text{gen,slow}}$ increases proportionally with the light intensity for low illumination levels ($< 1 \text{ mW/cm}^2$) and saturates for intensities above 1 mW/cm^2 . Similar results have been reported by Hashigami *et al.*²⁷ The proportional increase of $R_{\text{gen,slow}}$ found for very small light intensities would be expected from a recombination-enhanced process that is characterized by a proportional relationship between the defect generation rate and the recombination rate U . Since an illumination level of only 1 mW/cm^2 corresponds to a Fermi level splitting of several hundred millivolts and excess carriers concentrations in the vicinity of 10^{13} cm^{-3} , a precise study of $R_{\text{gen,slow}}$ as a function of the carrier concentration is only possible using electrical measurements, i.e., by successively increasing the minority-carrier (electron) concentration applying defined voltages to a p - n junction. Using solar cells made on Cz-Si as test devices, Bothe and Schmidt¹⁶ showed that the driving force of the defect formation is related to the *total* recombination rate and not to the *net* recombination rate as it had been expected before.²⁸ Their experimental results pointed towards a recombination-enhanced mechanism to be responsible for the defect formation, suggesting that the amount of energy released during a recombination event enhances the diffusion of the oxygen dimer. This interpretation is also capable of explaining the surprising experimental finding that a lifetime degradation can be observed under apparent equilibrium conditions (no voltage applied and complete darkness) at elevated temperatures ($> 300 \text{ K}$).¹⁶ With increasing temperature the increase in the minority-carrier concentration results in an increased absolute recombination rate and thus in a defect formation in the dark. The interpretation of an electronically stimulated defect formation is further supported by the results shown in Fig. 10 which rule out a simple charge state change model to describe the temperature dependence of the V_{50} voltage. Such a model had been proposed in an earlier study¹⁷ as a possible candidate to explain the asymptotic defect formation. According to theoretical calculations of Ewels,²⁹ the stable form of the neutral oxygen dimer is a staggered configuration. Hence, a staggered configuration has also been assumed for the B_sO_{2i} complex as a possible stable structure.⁶

Recently, the B_sO_{2i} model and its formation mechanism have been investigated theoretically using the AIMPRO spin-polarized density-functional theory code.³⁰ The calculations

showed that the two most stable configurations of B_sO_{2i} are a square ($B_sO_{2i}^{\text{sq}}$) and a staggered ($B_sO_{2i}^{\text{st}}$) form. The staggered configuration was found to be more stable when single positively charged, while the square form was found to be more stable when neutral. Furthermore, calculations of the ionization energies of the B_sO_{2i} complex revealed that the $B_sO_{2i}^{\text{sq}}$ configuration has a $(0/+)$ donor level in the upper half of the silicon band gap located somewhere between $E_C - 0.1 \text{ eV}$ and $E_C - 0.3 \text{ eV}$.³⁰ Thus, for temperatures around room temperature $B_sO_{2i}^{\text{sq}}$ is the most likely candidate responsible for the asymptotic degradation of the carrier lifetime in B-doped oxygen-rich silicon.

In the proposed defect formation model,⁶ the diffusivity of the oxygen dimer is a crucial parameter. Very different values for the migration energy of the oxygen dimer have been reported in the literature. While Ewels²⁹ calculated a migration energy of $\sim 1.3 \text{ eV}$, making the dimer virtually immobile at room temperature, Lee *et al.*²⁵ calculated a lower migration barrier of only 0.3 – 0.9 eV . Adey *et al.*³⁰ showed that the double positively charged oxygen dimer O_{2i}^{++} can diffuse very rapidly in crystalline silicon via a Bourgoin-Corbett mechanism by alternately capturing electrons and holes.^{31,32} By this mechanism the diffusion barrier of the dimer is reduced to 0.3 eV , which is close to the experimentally determined value of $E_{\text{gen,slow}} = (0.475 \pm 0.035) \text{ eV}$. Importantly, in this model the migration of the oxygen dimer would already proceed at room temperature, which is in perfect agreement with our experimental observations.

As can be seen from Fig. 9, $R_{\text{gen,slow}}$ does *not* depend on $[O_i]$. The explanation of this finding follows the argumentation from the formation of FeB pairs in silicon, where the defect formation rate does not depend on the interstitial iron concentration $[Fe_i]$ since the diffusing species Fe_i exists in a significantly smaller concentration compared to boron.³³ In our case, the diffusing species O_{2i}^{++} is present in a much lower concentration compared to B_s^- and thus a dependence of $R_{\text{gen,slow}}$ on $[O_i]$ may not be expected.

Studying the doping dependence of $R_{\text{gen,slow}}$ reveals a clear quadratic increase on the boron concentration $R_{\text{gen,slow}} \propto [B_s]^2$, as shown in Fig. 8. Adey *et al.*³⁰ assumed that $R_{\text{gen,slow}}$ is proportional to the initial O_{2i}^{++} concentration and deduced from this assumption that $R_{\text{gen,slow}}$ is proportional to $[B_s]^2$, as found experimentally. However, the assumption of Adey *et al.* also predicts $R_{\text{gen,slow}}$ to be proportional to the O_{2i} concentration. Thus, since the O_{2i} concentration is known to show a quadratic dependence on the interstitial oxygen concentration,²⁴ one would expect a quadratic increase of $R_{\text{gen,slow}}$ with $[O_i]$, which is in clear contradiction to our experimental finding shown in Fig. 9. One might also argue that Adey *et al.* have neglected the direct impact of boron on the defect formation rate since the higher the boron concentration the higher is the probability of an oxygen dimer to be captured. Such dependence also applies to FeB pairs in crystalline silicon.³³ In general, diffusion-limited pairing reactions with a high sticking probability, as is the case for Coulombic attraction between two oppositely charged ions, always show a linear dependence of the formation rate on the concentration of the immobile species.³⁴ As explained above, in the model of Adey *et al.*^{30,32} the diffusion of the O_{2i}^{++}

proceeds by alternately capturing electrons and holes. In this recombination-enhanced migration process the diffusion of the oxygen dimer critically depends on the hole concentration and thus is directly proportional to $[B_s]$. Following this line of arguments, a quadratic dependence of R_{gen} on $[B_s]$ may be predicted.³⁵ The advantage of this explanation over that proposed by Adey *et al.*³⁰ is that it does not contradict the experimental finding of $R_{\text{gen,slow}}$ being independent of the interstitial oxygen concentration.

The most likely configuration of the slowly forming defect center is the $[B_sO_{2i}^{\text{sq}}]^+$ configuration that acts as a Coulomb attractive center for electrons.^{30,32} This theoretical result agrees well with the experimentally determined electronic defect properties. By injection-level-dependent carrier lifetime measurements, Schmidt and Cuevas¹⁸ located the energy level of the slowly forming recombination center between $E_V+0.35$ and $E_C-0.45$ eV and determined a σ_n/σ_p ratio of ~ 10 , pointing towards a positively charged Coulomb center. Combining temperature-dependent carrier lifetime measurements under low-level injection conditions with injection-level-dependent carrier lifetime measurements, Rein and Glunz¹⁹ were able to pin down the energy level to $E_C-0.41$ eV. Furthermore, the temperature dependence of the low-level injection carrier lifetime could only be modeled by assuming a temperature-dependent electron-capture cross section $\sigma_n(T)=\sigma_{n0}T^\alpha$ with α between -1.5 and -2.0 . Such a decrease of the capture cross section with increasing temperature is expected for Coulomb attractive recombination centers.¹⁹

Since the initial carrier lifetime level can be fully recovered by annealing at 200°C for 10 min, a thermally activated annihilation process is expected. This expectation is confirmed by the experimental results shown in Fig. 13. The dynamic approach of Rein *et al.*¹⁷ as well as the static approach of Schmidt and Bothe⁶ yields the same result. From a linear fit to the measured data, an activation energy $E_{\text{ann,slow}}=(1.32\pm 0.05)$ eV is obtained for the annihilation process of the slowly forming defect center. A further analysis of the preexponential factor κ_0 yields a value of $\sim 10^{13}\text{ s}^{-1}$. Such a value is expected for a diffusion-limited process with $\kappa_0=\nu_0/n_j$, where $\nu_0\approx 10^{12}-10^{13}\text{ s}^{-1}$ is the vibrational frequency of an atom at a lattice site in the silicon host lattice and n_j is the number of jumps required for complete dissociation. The activation energy for the complete dissociation of the $[B_sO_{2i}^{\text{sq}}]^+$ complex has been calculated³⁰ to be $E_{\text{ann,slow}}\approx E_{\text{bind}}+E_{\text{mig}}$ with $E_{\text{bind}}=0.38$ eV being the binding energy between B_s^- and O_{2i}^{++} and $E_{\text{mig}}=0.86$ eV being the migration energy of the double positively charged oxygen dimer in the dark. The calculated activation energy $E_{\text{bind}}+E_{\text{mig}}=1.24$ eV for the dissociation of the slowly forming boron-oxygen complex is in excellent agreement with our experimentally determined value of 1.32 eV.

B. Fast initial degradation

As can be seen from Figs. 3 and 4, the normalized defect concentration N_τ corresponding to the fast-forming recombination center shows the same linear increase with the boron content and the same quadratic increase with the interstitial

oxygen concentration as the slowly forming center. Since for the slowly forming center these relations can be explained by the B_sO_{2i} model, we also assume the participation of one B_s and two O_i atoms in the fast initial degradation process. This assumption is supported by theoretical studies of Adey *et al.*^{30,36} who found that different stable B_sO_{2i} configurations do exist in crystalline silicon. Note that the carrier lifetime measurements used to determine N_τ of the fast-forming center have all been performed at a fixed injection level of $\eta=0.01$ since the fast-forming center mainly affects the carrier lifetime in the low-injection regime, as can be seen from Fig. 5.

According to the experimental results shown in Fig. 6, the formation of the fast-forming recombination center is a thermally activated process with a relatively low barrier energy of $E_{\text{gen,fast}}=(0.23\pm 0.02)$ eV. A more detailed analysis of the underlying formation mechanism reveals that a charge state change of a latent energy level $E_{\text{lat}}=E_V+(635\pm 20)$ meV results in the activation of the center responsible for the fast initial degradation. Applying different forward-bias voltages V_{appl} in the dark, the electron quasi-Fermi level is successively shifted towards the conduction band. As can be seen from Fig. 11, with increasing V_{appl} the resulting V_{OC} saturation values decrease. For small applied voltages ($V_{\text{appl}}<0.3$ V) no decrease in V_{OC} is observed, whereas the V_{OC} degradation saturates for $V_{\text{appl}}>0.6$ V, indicating a complete activation of the fast-forming recombination centers. Figure 12 shows the temperature dependence of the V_{50} voltage, required to activate 50% of the maximum defect concentration, for different doping concentrations. Simultaneously fitting all three curves allows to determine the position of the latent energy level $E_{\text{lat}}=E_F+qV_{50}$.

Taking into account our experimental results as well as the results of the *ab initio* calculations of Adey *et al.*^{30,32} our suggestion for the fast defect formation process is a charge state change of a latent B_sO_{2i} complex $C(C^+\rightarrow C^0)$ accompanied by a thermally activated structural change with an activation energy of ~ 0.23 eV to a structure $D(C^0\rightarrow D^0)$, possibly followed by a charge state change $D^0\rightarrow D^+$. The occurrence of the last step critically depends on the position of the Fermi level and the actual position of the energy level of structure D. As can be seen from the analysis of the SRH lifetime shown in Fig. 5, the recombination center associated with the fast initial degradation process is characterized by a σ_n/σ_p ratio of ~ 100 , supporting a D^+ or even a D^{++} state.

For a complete understanding of the formation mechanism of the slowly forming defect center it is important to know whether the fast-forming center is a precursor of the subsequently slowly forming B_sO_{2i} complex or if both centers form independently of each other. In order to clarify this, we have designed a two-step experiment to study the decrease in the V_{OC} as a function of V_{appl} . In the first step, we compare (i) the impact of an applied voltage capable of shifting the electron quasi-Fermi level E_{Fn} across E_{lat} with (ii) an applied voltage that is not able to rise the electron quasi-Fermi level across E_{lat} . An applied voltage of $V_{\text{appl}}=0.4$ V does not shift the electron quasi-Fermi level across E_{lat} and hence, as can be seen from Fig. 16, a fast decrease in V_{OC} cannot be observed. In contrast, the application of V_{appl}

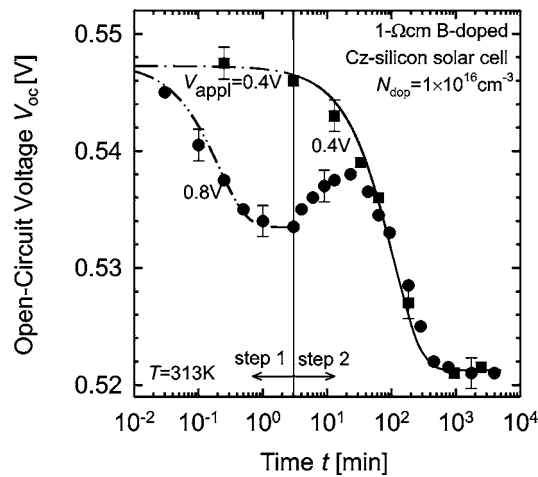


FIG. 16. Measured decrease in the open-circuit voltage V_{OC} of a Cz-Si MIS n^+p solar cell with a base doping concentration of $N_{dop} = 1.5 \times 10^{16} \text{ cm}^{-3}$ due to the application of an applied voltage V_{appl} in the dark. For the measurement of V_{OC} , the solar cell is illuminated with light from a halogen lamp with an intensity of only 10 mW/cm^2 for 2 s. The formation of the fast-forming center can intentionally be allowed ($V_{appl} = 0.8 \text{ V}$, circles) or suppressed ($V_{appl} = 0.4 \text{ V}$, squares). In both cases the slowly forming center limits the final V_{OC} value and forms in the same way, proving that the fast and the slow defect formation are independent processes.

$= 0.8 \text{ V}$ for 3 min results in a full activation of the fast-forming center due to the shift of E_{Fn} across E_{lat} . In the second step, V_{appl} is chosen to be (i) sufficiently large to result in the formation of the slowly forming center but (ii) small enough not to result in the formation of the fast-forming recombination center. As known from previous investigations,¹⁶ both conditions are fulfilled for $V_{appl} = 0.4 \text{ V}$. In case (i) (filled squares, $V_{appl} = 0.4 \text{ V}$ for steps 1 and 2), the measured decrease in V_{OC} follows a pure mono-exponential decay over the entire range. In case (ii) (filled circles, $V_{appl} = 0.8 \text{ V}$ during step 1, $V_{appl} = 0.4 \text{ V}$ during step 2), the open-circuit voltage in the beginning of step 2 is limited by the fully activated fast-forming center. Interestingly, the drop of E_{Fn} below E_{lat} results in an annihilation of the fast-forming center, as indicated by the increase in V_{OC} during step 2. However, in the asymptotic case, we observe a convergence of the two curves (squares and circles), indicating that the open-circuit voltage is ultimately limited by the formation of the slowly forming boron-oxygen complex only. These results clearly prove that both recombination centers are formed completely independent of each other and that the fast-forming center is not a precursor of the subsequently slowly forming defect.

Aiming at understanding the annihilation process of the fast-forming center observed in the two-step experiment at a relatively low temperature of 313 K, we study the V_{OC} recovery after complete activation of the fast-forming center as a function of temperature between 300 and 450 K. It has to be stressed that this analysis starts from a level where *only* the fast-forming center is activated. Thus, all results can be attributed to the fast-forming defect center alone. As shown in Fig. 14, the annihilation proceeds via two stages. During the first stage, an intermediate level is reached, while during the second stage a complete recovery of the initial V_{OC} level is observed. Below $\sim 330 \text{ K}$ only the intermediate level is

reached within 10^6 s , whereas for temperatures above $\sim 425 \text{ K}$ the annihilation taking place in stage one cannot be measured adequately. The reason for this becomes clear when analyzing the defect annihilation rates corresponding to the two stages as a function of temperature as shown in Fig. 15. While the energy barrier of the first stage is only $E_{ann.fast.1} = (0.32 \pm 0.02) \text{ eV}$, the energy barrier of the second stage is significantly larger $E_{ann.fast.2} = (1.36 \pm 0.08) \text{ eV}$. Thus, the annihilation process resulting in the intermediate state proceeds much faster compared to the annihilation resulting in a complete recovery. An analysis of the preexponential factors κ_0 of the two processes yields values of $\sim 10^3 \text{ s}^{-1}$ for the first and $\sim 10^{13} \text{ s}^{-1}$ for the second stage. Thus, a diffusion-limited process can be ruled out for the first annihilation stage, making a configurational change most likely. This conclusion is supported by the result of the experiment shown in Fig. 16. As can be seen from Fig. 16, the annihilation of the fast-forming center starts immediately after shifting the electron quasi-Fermi level below the latent energy state (i.e., applying only 0.4 V rather than 0.8 V during step 2).

The preexponential factor of $\kappa_0 \approx 10^{13} \text{ s}^{-1}$ as well as the barrier energy of $(1.36 \pm 0.08) \text{ eV}$ of the second annihilation stage are very similar to the corresponding values measured for the annihilation of the slowly forming center. When plotting $R_{ann.slow}$ and $R_{ann.fast.2}$ in one Arrhenius plot, one even finds that for the same doping concentration both curves lie perfectly on top of each other. A possible explanation might be that the first annihilation stage is a structural change of the fast-forming boron-oxygen complex $B_sO_{2i}^{fast}$ into the configuration of the slowly formed complex $B_sO_{2i}^{slow}$. Since the capture cross-section ratio σ_n/σ_p of the $B_sO_{2i}^{slow}$ center is lower by one order of magnitude, the structural change results in a less recombination-active center with a smaller electron affinity and thus in a carrier lifetime increase. In Fig. 14, this corresponds to the decrease in N_{VOC} during the first annihilation stage. During the second stage, the annihilation proceeds in the same way as it was observed for the annihilation of the slowly forming center, resulting in a complete recovery of the initial lifetime as discussed in Sec. IV A.

V. CONCLUSION

The simultaneous presence of boron and oxygen in crystalline silicon results in the formation of recombination-active defect centers under illumination or the injection of minority carriers via a p - n junction. The formation of these recombination centers results in a pronounced degradation of the bulk carrier lifetime that can be monitored by carrier lifetime and open-circuit voltage measurements. Using time-resolved lifetime and open-circuit voltage measurements, we have shown that the decrease of the carrier lifetime proceeds via a two-step process with a fast initial decay on a time scale of seconds to minutes followed by a subsequent slowly decay on a time scale of minutes to hours. The concentration of the fast as well as that of the slowly forming defect center exhibits a linear dependence on the substitutional boron and a quadratic dependence on the interstitial oxygen concentration. This finding suggests the direct involvement of one B_s

TABLE I. Properties of the boron-oxygen-related recombination centers in crystalline silicon corresponding to the fast initial and the subsequent asymptotic slow degradation process.

	Fast process	Slow process
N_τ	$\propto [\text{O}_i]^{(2.0 \pm 0.2)}$ $\propto [\text{B}_s]^{(1.05 \pm 0.05)}$	$\propto [\text{O}_i]^{(1.9 \pm 0.1)}$ $\propto [\text{B}_s]^{(1.05 \pm 0.05)}$
R_{gen}	$\propto [\text{O}_i]^0$ $\propto [\text{B}_s]^{(2.00 \pm 0.03)}$	$\propto [\text{O}_i]^0$ $\propto [\text{B}_s]^{(2.00 \pm 0.03)}$
E_t	$E_C - (0.60 \pm 0.25) \text{ eV}$	$E_C - 0.41 \text{ eV}^a$
σ_n/σ_p	100 ± 10	10 ± 1^a
E_{gen}	$(0.23 \pm 0.02) \text{ eV}$	$(0.475 \pm 0.035) \text{ eV}$
E_{ann}	$(0.32 \pm 0.02) \text{ eV}$ (stage 1) $(1.36 \pm 0.08) \text{ eV}$ (stage 2)	$(1.32 \pm 0.05) \text{ eV}$

^aReferences 18 and 19.

and two O_i atoms in both centers. Our suggestion of a B_sO_{2i} complex in different configurations as possible candidates for the fast- and the slowly forming recombination centers is supported by recent *ab-initio* calculations which revealed that different stable B_sO_{2i} configurations do exist in crystalline silicon.

The electronic defect parameters and the formation mechanisms of the two boron-oxygen centers are different. While the fast-forming center with a σ_n/σ_p ratio of ~ 100 mainly affects the injection-level-dependent carrier lifetime in the low-injection regime, the slowly forming center with $\sigma_n/\sigma_p \approx 10$ results in a lifetime degradation over the entire injection range. The formation of the fast-forming center is triggered by shifting the electron quasi-Fermi level across a defined energy level at $E_V + 635 \text{ meV}$, while the formation of the slowly forming center can be explained by a fast-diffusing double positively charged oxygen dimer O_{2i}^{++} that is captured by a substitutional boron atom B_s^- , resulting in the recombination-active Coulomb center $\text{B}_s\text{O}_{2i}^+$.

Based on a detailed analysis of the open-circuit voltage degradation of Cz-silicon solar cells as a function of different applied forward-bias voltages we have shown that the two B_sO_{2i} centers form simultaneously and that the fast-forming center is not a precursor of the slowly forming one, i.e., both centers form completely independent of each other. The final carrier lifetime is limited by the slowly forming center only, which therefore is the relevant recombination center limiting the device performance of silicon solar cells made on boron-doped oxygen-contaminated crystalline silicon. Finally all data of the fast and the slowly forming defect center are summarized in Table I.

ACKNOWLEDGMENTS

The authors wish to thank D.W. Palmer for stimulating and informative discussions and R. Brendel for his continuous support and encouragement. S. W. Glunz is acknowledged for providing PERL silicon solar cells with different base doping concentrations and M. Heuer as well as M. Steinhof for sample preparation and solar cell processing.

Funding was provided by the State of Lower Saxony and the German Ministry of Education and Research (BMBF) under Contract No. 01SF0009. The ISFH is a member of the German Forschungsverbund Sonnenenergie (FVS).

- ¹H. Fischer and W. Pschunder, *Proceedings of the tenth IEEE Photovoltaic Specialists Conference* (IEEE, New York, 1973), p. 404.
- ²J. Knobloch *et al.*, *Proceedings of the 13th European Photovoltaic Solar Energy Conference* (Stephens, Bedford, 1995), p. 9.
- ³J. Schmidt, A. G. Aberle, and R. Hezel, *Proceedings of the 26th IEEE Photovoltaic Specialists Conference* (IEEE, New York, 1997), p. 13.
- ⁴J. Schmidt, *Solid State Phenom.* **95–96**, 187 (2004).
- ⁵S. W. Glunz, S. Rein, W. Warta, J. Knobloch, and W. Wettling, *Proceedings of the Second World Conference on Photovoltaic Solar Energy* (European Commission, Ispra, Italy, 1998), p. 1343.
- ⁶J. Schmidt and K. Bothe, *Phys. Rev. B* **69**, 024107 (2004).
- ⁷S. Rein, S. Diez, R. Falster, and S. W. Glunz, *Proceedings of the Third World Conference on Photovoltaic Solar Energy* (WCPEC-3 Organizing Committee, Oosaka, Japan, 2003), p. 1048.
- ⁸K. Bothe, J. Schmidt, and R. Hezel, *Proceedings of the Third World Conference on Photovoltaic Solar Energy* (WCPEC-3 Organizing Committee, Oosaka, Japan, 2003), p. 1077.
- ⁹H. Hashigami, M. Dhamrin, and T. Saitoh, *Proceedings of the Third World Conference on Photovoltaic Solar Energy* (WCPEC-3 Organizing Committee, Oosaka, Japan, 2003), p. 1116.
- ¹⁰T. Lauinger, J. Schmidt, A. G. Aberle, and R. Hezel, *Appl. Phys. Lett.* **68**, 1232 (1996).
- ¹¹J. Knobloch, A. Noel, E. Schäffer, U. Schubert, F. J. Kamerewerd, S. Klüßmann, and W. Wettling, *Proceedings of the 23rd IEEE Photovoltaic Specialists Conference* (IEEE, New York, 1993), p. 271.
- ¹²A. Metz and R. Hezel, *Proceedings of the 26th IEEE Photovoltaic Specialists Conference* (IEEE, New York, 1997), p. 283.
- ¹³K. Bothe, J. Schmidt, and R. Hezel, *Proceedings of the 29th IEEE Photovoltaic Specialists Conference* (IEEE, New York, 2002), p. 194.
- ¹⁴W. Shockley and W. T. Read, *Phys. Rev.* **87**, 835 (1952).
- ¹⁵R. N. Hall, *Phys. Rev.* **87**, 387 (1952).
- ¹⁶K. Bothe and J. Schmidt, *Appl. Phys. Lett.* **83**, 1125 (2003).
- ¹⁷S. Rein, T. Rehrl, W. Warta, S. W. Glunz, and G. Willeke, *Proceedings of the 17th European Photovoltaic Solar Energy Conference* (WIP, Munich, 2001), p. 1555.
- ¹⁸J. Schmidt and A. Cuevas, *J. Appl. Phys.* **86**, 3175 (1999).
- ¹⁹S. Rein and S. W. Glunz, *Appl. Phys. Lett.* **82**, 1054 (2003).
- ²⁰S. W. Glunz, E. Schäffer, S. Rein, K. Bothe, and J. Schmidt, *Proceedings of the Third World Conference on Photovoltaic Solar Energy* (WCPEC-3 Organizing Committee, Oosaka, Japan, 2003), p. 919.
- ²¹J. Schmidt, K. Bothe, and R. Hezel, *Proceedings of the 29th IEEE Photovoltaic Specialists Conference* (IEEE, New York, 2002), p. 178.
- ²²K. Bothe, R. Sinton, and J. Schmidt, *Prog. Photovoltaics* **13**, 287 (2005).
- ²³D. Macdonald, P. N. K. Deenapanray, A. Cuevas, S. Diez, and S. W. Glunz, *Solid State Phenom.* **108–109**, 497 (2005).
- ²⁴L. I. Murin, T. Hallberg, V. P. Markevich, and J. L. Lindström, *Phys. Rev. Lett.* **80**, 93 (1998).
- ²⁵Y. L. Lee, J. von Boehm, M. Pesola, and R. M. Nieminen, *Phys. Rev. Lett.* **86**, 3060 (2001).
- ²⁶J. L. Lindström and T. Hallberg, *Proceedings of the NATO Advanced Research Workshop on Early Stages of Oxygen Precipitation in Silicon* (Kluwer, Dordrecht, 1996), p. 41.
- ²⁷H. Hashigami, Y. Itakura, and T. Saitoh, *J. Appl. Phys.* **93**, 4240 (2003).
- ²⁸J. Knobloch, S. W. Glunz, D. Biro, W. Warta, E. Schäffer, and W. Wettling, *Proceedings of the 25th IEEE Photovoltaic Specialists Conference* (IEEE, New York, 1996), p. 405.
- ²⁹C. P. Ewels, Ph.D. thesis, University of Exeter, 1997.
- ³⁰J. Adey, R. Jones, D. W. Palmer, P. R. Briddon, and S. Öberg, *Phys. Rev. Lett.* **93**, 055504 (2004).
- ³¹J. C. Bourgoin and J. W. Corbett, *Phys. Lett.* **38A**, 135 (1972).
- ³²J. Adey, Ph.D. thesis, University of Exeter, 2005.
- ³³L. C. Kimerling and J. L. Benton, *Physica B & C* **116**, 297 (1983).
- ³⁴H. Reiss, C. S. Fuller, and F. J. Morin, *Bell Syst. Tech. J.* **35**, 535 (1956).
- ³⁵D. W. Palmer, K. Bothe, and J. Schmidt (unpublished).
- ³⁶J. Adey, R. Jones, and D. W. Palmer (private communication).